Ligand-Field Control and Hydrogen Bonding as Design Elements in the Assembly and Crystallization of Poly(azolyl)borate–Metal Complexes: Chelate Complexes versus Coordination Polymers and Symmetrical versus Distorted Grid Sheets

Christoph Janiak,* Tobias G. Scharmann, Wulf Günther, Frank Girgsdies, Holger Hemling, Winfried Hinrichs, and Dieter Lentz

Dedicated to Prof. Dr. Herbert Schumann on the occasion of his 60th birthday

Abstract: The 1- and 2-D coordination polymers $[Mn\{HB(C_2H_2N_3)_3\}_2(H_2O)_2]\cdot 4H_2O$ (**11**) and $[Ni\{H_2B(CHN_4)_2\}_2(NH_3)_2]$ (**13**), respectively, and the chelate complex $[Ni\{H_2B(C_2H_2N_3)_2\}_2(H_2O)_2]\cdot 2H_2O$ (**12**) were synthesized and structurally characterized. The compounds contain ambidentate poly(azolyl)borato ligands (azolyl = triazolyl or tetrazolyl), which can chelate or bridge metal centers. The metal–ligand structures in **11**–**13** differ from the known coordination modes of the poly(azolyl)borates towards other metal centers. We describe how a change in the metal and/or the conditions of crystallization affects the ligand-field stabilization energy and favors one type of nitrogen donor atom over the other for the poly(triazolyl)borato ligands. The crystal structures of **11** and **12** contain additional water of crystallization; this leads to hydrogen-bonded solvent substructures. In the case of the bis(tetrazolyl)borato ligand the water substructure is shown to function as a "reinforcing bar" that symmetrizes the metal–ligand grid sheet.

Keywords
chelate ligands · coordination · hydrogen bonds · ligand fields · polymers

Introduction

While the versatile poly(pyrazolyl)borato ligands form exclusively molecular (chelate) complexes as depicted in **1** and **2**,[1] the novel hydrotris(1,2,4-triazolyl)- and dihydrobis(1,2,4-triazolyl)borate (**3** and **4**, respectively) and dihydrobis(tetrazolyl)borate (**5**)[2] ligands with their multiple bonding centers can, in principle, chelate or bridge metal centers. The latter results in structurally diverse coordination polymers. Furthermore, the nitrogen atoms which are not utilized for metal coordination tend to engage in hydrogen bonding with solvate molecules; this leads to the formation of solvent-stabilized crystal phases with interesting water substructures.[3–6] Tris(triazolyl)borate (**3**) has been found to function as a tris-chelating ligand by coordination through the endodentate nitrogen

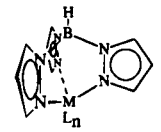

1

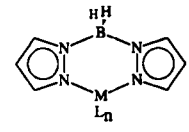

2

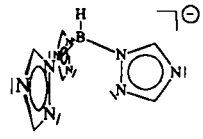

3

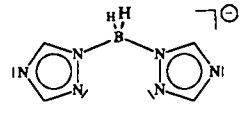

4

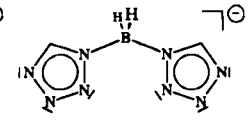

5

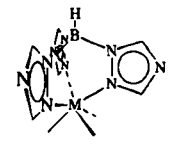

(M = Fe, Co, Ni, Cu, Zn)

6

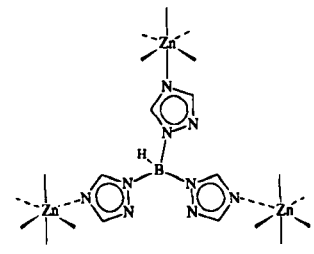

7

[*] Dr. C. Janiak, Dipl.-Chem. T. G. Scharmann, Dr. W. Günther, Dipl.-Chem. F. Girgsdies, Dr. H. Hemling
Institut für Anorganische und Analytische Chemie
Technische Universität Berlin
Strasse des 17. Juni 135, 10623 Berlin (Germany)
Telefax: Int. code + (30) 314-22168

Dr. W. Hinrichs
Institut für Kristallographie, Freie Universität Berlin
Takustrasse 6, 14195 Berlin (Germany)

Dr. D. Lentz
Institut für Anorganische und Analytische Chemie, Freie Universität Berlin
Fabeckstr. 34–36, 14195 Berlin (Germany)

  0947-6539/95/0109-0637 $ 10.00+.25/0

donors to metals such as iron, cobalt,[3] nickel,[5] copper,[7] and zinc to form complexes (**6**).[4] In addition, it has been demonstrated that the zinc complex of **3** also exists as a linkage isomer of **6**, as a three-dimensional coordination polymer formed by the bridging of three zinc centers by the exodentate nitrogen atoms of the borate (**7**).[4] The bis(triazolyl)borato ligand (**4**) has so far been found only to exhibit bridging coordination through the exodentate nitrogens towards manganese and copper to give highly solvated 2- and 1-D coordination polymers, respectively (**8** and **9**).[5] Bridging coordination resulting in 2-D coordination polymers is also the sole structural type so far found in the transition-metal complexes of **5** (**10**).[6] (The hydrogen bonds between water of crystallization and the "free" nitrogen atoms have not been included in the formulae **6**–**10** for clarity.)

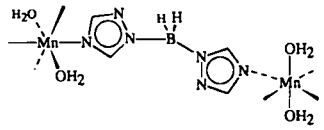

8

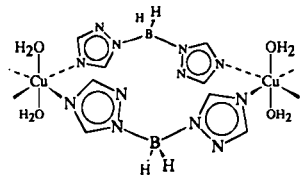

9

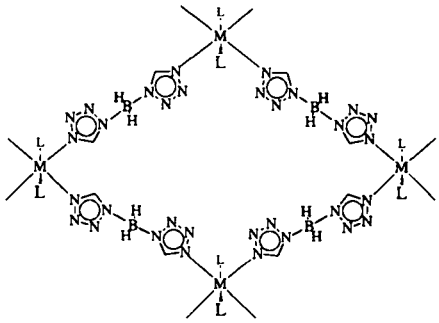

10 (M = Mn, Fe, Co, Zn, Cd; L = H_2O; symmetrical)
10' (M = Cu; L = NH_3; distorted)

Up to now, the bridging action of **4** and **5** has been explained on electrostatic grounds,[3,4] and the chelating, endodentate coordination observed with **3** on the basis of the "chelating effect" overcoming the charge-dictated ligating requirements.[5] New results presented here indicate, however, that the self-assembly process during crystallization depends on other factors as well. These factors, or the control of the assembly process from ionic building blocks with the help of the ligand field of the metal, are the subject of this paper; the design of solids through the assembly of structurally defined subunits is a challenge for chemists.[8]

Results

Syntheses and properties of 11–13: The potassium salt of the hydrotris(triazolyl)borato anion (**3**) reacted with manganese(II) chloride in water to form diaquabis[μ-hydrotris(triazolyl)-borato]manganese(II) [Eq. (1)]. Upon slow diffusion of the reactant solutions, the manganese compound **11**, including water of crystallization, was obtained as colorless crystals directly from the reaction mixture in good yield. Under the same conditions,

$$MnCl_2 + 2K[HB(C_2H_2N_3)_3] \longrightarrow \underset{\mathbf{11}}{{}^{1}_{\infty}\{[Mn\{HB(C_2H_2N_3)_3\}_2(H_2O)_2]\cdot 4H_2O\}} + 2KCl \quad (1)$$

(hydrated) nickel(II) chloride and ligands **4** and **5** furnished amorphous blue-violet powders. These nickel compounds were soluble in aqueous ammonia (presumably with formation of nickel–ammine complexes) from which pink-violet crystals of **12** (needle-shaped) [Eq. (2)] and **13** [Eq. (3)] could be grown upon slow solvent evaporation.[9] In line with the crystallization

$$NiCl_2 + 2K[H_2B(C_2H_2N_3)_2] \xrightarrow[2)\ NH_3]{1)\ H_2O} \underset{\mathbf{12}}{[Ni\{H_2B(C_2H_2N_3)_2\}_2(H_2O)_2]\cdot 2H_2O} + 2KCl \quad (2)$$

$$NiCl_2 + 2K[H_2B(CHN_4)_2] \xrightarrow[2)\ NH_3]{1)\ H_2O} \underset{\mathbf{13}}{{}^{2}_{\infty}\{[Ni\{H_2B(CHN_4)_2\}_2(NH_3)_2]\}} + 2KCl \quad (3)$$

from ammonia, complex **13** could be obtained in a crystalline form directly from the reaction mixture when the diffusion method was used with water or methanol as a solvent and hexaamminenickel(II) chloride as a starting material [Eq. (4)].

$$\underset{\mathbf{5}}{[Ni(NH_3)_6]Cl_2} + 2K[H_2B(CHN_4)_2] \longrightarrow \underset{\mathbf{13}}{{}^{2}_{\infty}\{[Ni\{H_2B(CHN_4)_2\}_2(NH_3)_2]\}} + 2KCl \quad (4)$$

X-ray structural investigations show that crystals of **11** and **12** contain four and two water molecules of crystallization per formula unit, respectively. Crystals of **11** do not lose this incorporated solvent when removed from the aqueous phase, or only eliminate it very slowly, while crystals of **12** quickly lose water of crystallization. Except for the solubility of **12** and **13** in aqueous ammonia, the complexes (**11**–**13**) are insoluble in aqueous or organic solvents once they have formed. For **11** this is especially noteworthy as the analogous molecular iron, cobalt, nickel, and zinc complexes are at least sparingly soluble in water. Aside from the loss of water of crystallization, the compounds are thermally stable to over 500 °C (**11**), 260 °C (**12**), and 250 °C (**13**). The infrared spectra reflect the ligand moieties, yet they exhibit distinct differences from the spectra of the structurally authenticated homologues, **6** and **8**–**10**. In the case of **13** the differences with respect to **10** are illustrated in Figure 1. The obvious splitting of the C–H and B–H stretching frequencies (around 3150 and 2480 cm^{-1}, respectively) indicates a lower site symmetry of the borato ligand in **13** by comparison with the solid-state structure of **10**, where both triazolyl rings of the borate are symmetry-related.[6] The lower symmetry in **13** is indeed verified by the crystal structure analysis (see below).

A mass spectrum (EI) could only be obtained from **11**, and is attributed to the tris-chelating potential of the ligand **3**. The ML_2 ion [L = $HB(C_2H_2N_3)_3$] and other metal-containing fragments are high in abundance, with the former even being the

0947-6539/95/0109-0638 $ 10.00+.25/0 Chem. Eur. J. 1995, 1, No. 9

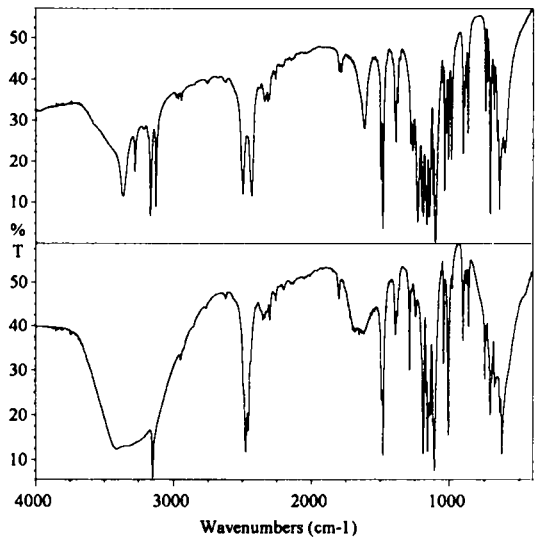

Fig. 1. Infrared spectra (KBr pellets, % transmission) of the nickel complex **13** (top) and the zinc complex [6] (bottom) of the bis(tetrazolyl)borato ligand (**5**).

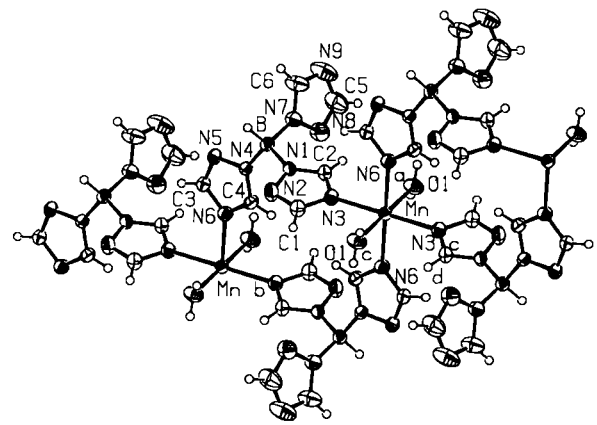

Fig. 2. Metal coordination and section of the linear chain structure with the atomic numbering scheme in **11** (PLATON-TME [11], 50% probability ellipsoids). The water of crystallization is not shown. Selected distances (Å) and angles (°): Mn–O1 2.197(2), Mn–N3 2.255(2), Mn–N6a/d 2.250(2), O1-Mn-O1c 180, O1-Mn-N3 89.47(9), O1-Mn-N3c 90.53(9), O1-Mn-N6a 87.59(9), O1-Mn-N6d 92.41(9), N3-Mn-N6d 90.79(9), N3-Mn-N6d 89.21(9). Symmetry transformations: $a = x-1, y, z$; $b = x+1, y, z$; $c = -x+1, -y+1, -z+1$; $d = -x+2, -y+1, -z+1$.

base peak at higher temperature. The fragmentation pattern corresponds to those of the other binary metal complexes of **3**.[5, 7] Attempts to study the bis(azolyl)borato systems by other methods (FAB, CI) have so far failed.

Temperature-variable magnetic measurements of **11**–**13** show normal paramagnetic Curie–Weiss behavior in the temperature range measured (14–300 K). In the polymeric complexes **11** and **13** there is no magnetic coupling transmitted through the ligand, nor is there a through-space interaction of the metal centers (shortest M–M contacts are 8.91/9.16 Å for **11** and 7.80/7.86 Å for **13**). The magnetic moments are temperature-independent within experimental error and lie within the range typically observed for d^5 (high-spin, $\mu = 5.7-6.0\,\mu_B$) or d^8 complexes ($\mu = 2.9-3.9\,\mu_B$, calculated spin-only value $\mu = 2.83\,\mu_B$).[10]

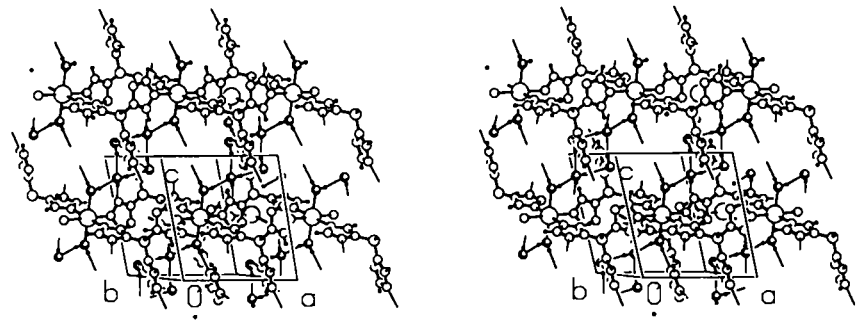

Fig. 3. Stereo plot of the crystal structure of **11** (crossed circles = oxygen atoms) (PLUTON [11]).

X-ray crystal structure of 11: Compound **11** is a one-dimensional coordination polymer with a linear chain structure. Here and in the structures of **12** and **13** the metal centers are octahedrally coordinated, with a coordination polyhedron formed from four nitrogen atoms of the (azolyl)borato ligands and two *trans*-coordinated solvent ligands (Fig. 2). In **11** the manganese ions are bridged by two borato ligands, each through the exodentate donor atoms of the triazolyl rings. The third triazolyl ring of the borate is not utilized for the metal coordination and only involved in the hydrogen bonding network. The feature of a "free" azolyl ring makes this manganese structure unique among the hitherto investigated modified poly(azolyl)borato structures. In all other structurally characterized poly(triazolyl)- or bis(tetrazolyl)borato complexes, at least one nitrogen donor from each azolyl ring coordinates to the metal;[3–7] sometimes two do so, as in the structure of the recent silver complex of **3**.[12]

A further important aspect in the discussion of the crystal structure of **11** is the stabilization of the crystal phase by solvent molecules, as has often been observed in metal structures of the novel poly(azolyl)borates **3**–**5**.[3–7] Figures 3 and 4 illustrate the incorporation of the four water molecules of crystallization as a tetramer with homodromic hydrogen bonds.[13] These water clusters are hydrogen-bonded further to the endodentate nitrogen atoms and to the metal-bound aqua ligands. The second hydrogen atom of the aqua ligand bridges the exodentate N atom of a free triazolyl ring. The utilization of all (O)–H atoms in hydrogen bonding allows the unproblematic location and refinement of these hydrogen atoms in the room temperature structure and explains the slow loss of the water of crystallization upon drying. We note also that C–H···O hydrogen bonds are formed between two of the manganese-coordinated triazolyl rings and the coplanar aqua ligands (Table 1 lists the lengths and angles of the hydrogen bonds). The aspect of C–H···O bonding and its importance for molecular alignment[14] in the crystal structures of the poly(azolyl)borates is, however, still under investigation, and a comparative account will be published later. The crystal of **11** was taken from a batch which had been stored under water for several months. In view of the known slow transformation of the analogous zinc complex from a molecular chelate to a 3-D coordination polymer (**6** to **7**)[4] and in the light of a mass spectrum typical of a molecular compound, the possibility of a second (molecular) crystal phase, or in other words, the representative nature of the single crystal

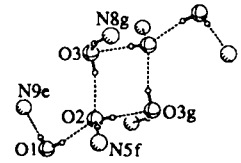

Fig. 4. Hydrate structure in **11**. Distances and angles of the hydrogen-bonding scheme are listed in Table 1.

Table 1. Hydrogen-bonding scheme in **11** [a] (distances in Å, angles in °).

D–H···A	D···A	D–H	H···A	D-H-A
O1–H12···O2	2.750(3)	0.83(4)	1.94(4)	166(4)
O1–H11···N9e	2.779(4)	0.87(4)	1.91(4)	169(4)
O2–H22···O3g	2.866(5)	0.89(5)	1.98(5)	177(4)
O2–H21···N5f	2.853(3)	0.88(4)	1.99(4)	170(4)
O3–H32···O2	2.874(4)	0.87(4)	2.01(4)	173(4)
O3–H31···N8g	2.987(4)	0.88(4)	2.14(4)	161(4)
C1–H1···O1c	3.323(4)	0.93(4)	2.86(4)	112(4)
C2–H2···O1	3.313(4)	0.92(4)	2.89(4)	110(4)

[a] The hydrate structure is shown in detail in Figure 4. Symmetry operations for equivalent atoms: $c = -x+1, -y+1, -z+1$; $e = -x+2, -y+2, -z+2$; $f = -x+1, -y, -z+1$; $g = -x+2, -y+1, -z+2$. All other O···O contacts are longer than 4.0 Å, O···N contacts longer than 3.7 Å. [b] D = donor, A = acceptor.

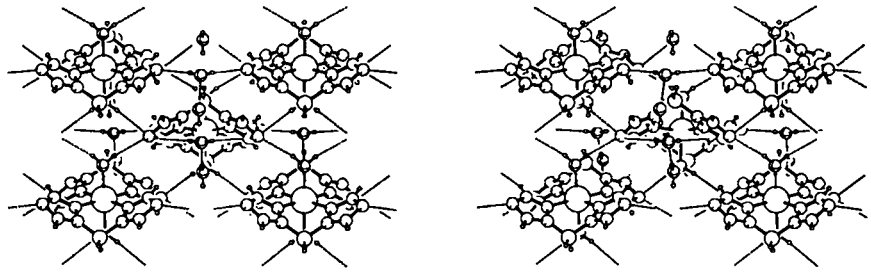

Fig. 7. Stereo view of the crystal structure of **12** along *b*. Dashed lines symbolize the hydrogen bonds between the H_2O molecules and the exodentate nitrogen atoms (PLUTON [11]).

with respect to the bulk material, had to be investigated. A powder diffraction study (Fig. 5) proved the identity of the single crystal with the bulk material as well as with a freshly prepared sample. Thus, no intermediate molecular chelate complex is formed in the case of **11**, unlike that of the zinc complex (**6**).

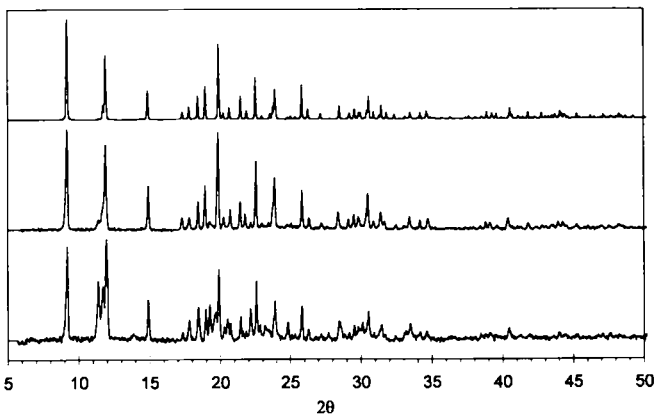

Fig. 5. X-ray powder pattern of a freshly prepared sample of **11** (middle), a sample stored under water for several months (bottom), and simulation (top) from the single crystal data [15]. The diffractogram of the aged sample shows additional peaks due to oxidized, brown Mn(IV) impurities.

X-Ray crystal structure of 12: The structural analysis of **12** shows the formation of a molecular chelate complex (Fig. 6) whose crystal structure is again stabilized by incorporated water (Figs. 7 and 8). The low-temperature water substructure can be described as being made up of H_2O dimers, with one of the molecules bridging exodentate nitrogens of different complex molecules with its hydrogen atoms. The aqua ligands also form bridges between N atoms with their hydrogens. No bridge between the aqua ligands and the water of crystallization could be found from the localized hydrogen atoms. At room temperature, however, such a connection may be possible, since one of the water molecules of crystallization (O3) still possesses a free hydrogen. In the "frozen" structure this oxygen is just 3.05 Å away from an aqua ligand (O2). Table 2 contains the lengths and angles of the hydrogen bonds.

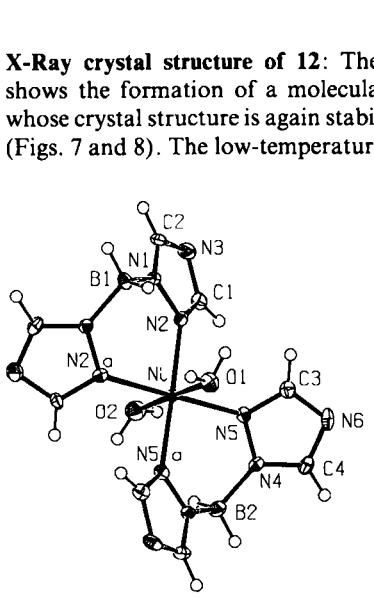

Fig. 6. Molecular structure of $[Ni\{H_2B(C_2H_2N_3)_2\}_2(H_2O)_2]$ in **12** with the atom numbering scheme (PLATON-TME [11], 50% probability ellipsoids). Selected distances (Å) and angles (°): Ni–O1 2.096(6), Ni–O2 2.112(6), Ni–N2 2.120(3), Ni–N5 2.125(4), O1-Ni-O2 178.3(2), N2a-Ni-N2 88.5(2), N5a-Ni-N5 89.9(2), N2-Ni-N5 90.8(1), N2-Ni-N5a 179.1(2), O-Ni-N 86.8(1)–93.8(1). Symmetry transformation: $a = -x, y, z$.

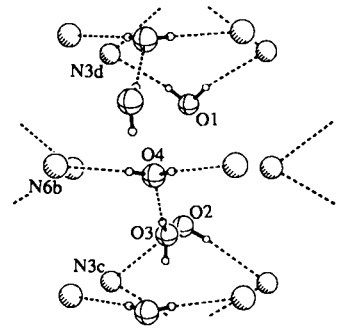

Fig. 8. Hydrate structure in **12**. Distances and angles of the hydrogen-bonding scheme are listed in Table 2.

Table 2. Hydrogen-bonding scheme in **12** [a] (distances in Å, angles in °).

D–H···A	D···A	D–H	H···A	D-H-A
O1–H11···N3d	3.151(6)	0.88(3)	2.32(4)	157(7)
O2–H21···N3c	3.376(6)	0.89(3)	2.49(3)	172(8)
O3–H31···O4	2.777(9)	0.83(3)	1.97(5)	164(13)
O4–H41···N6b	2.951(4)	0.83(3)	2.15(3)	164(7)

[a] The hydrate structure is shown in Figure 8. Symmetry operations for equivalent atoms: $b = -x+0.5, y+0.5, z$; $c = -x+0.5, -y+0.5, z-0.5$; $d = -x+0.5, -y+0.5, z+0.5$. The distance O2···O3 is 3.051(7) Å, without the presence of a hydrogen at 160 K. All other relevant O···O contacts are longer than 3.8, O···N contacts longer than 3.5 Å. [b] D = donor, A = acceptor.

The bis(triazolyl)borate (**4**) functions as a bidentate chelate ligand here, with the endodentate nitrogen atoms as donors. Comparison of the Ni–O and Ni–N bond lengths reveals only a small distortion of the pseudooctahedral coordination sphere. The ligand arrangement in the molecular structure (Fig. 6) leads one to expect an inversion symmetry at the nickel center. However, the normalized structure factor amplitudes point to an acentric space group. Of the space groups possible according to the systematic absences only $Cmc2_1$ permitted successful refinement. The heavy atoms in **12** have a pseudohexagonal symmetry (Fig. 9), so that the data set was at first (erroneously) recorded in the hexagonal setting. However, no refinement was possible in this crystal system—the arrangement of the ligands demanded an orthorhombic setup. Furthermore, Figure 9 illustrates the presence of channels which extend along *c* through the lattice and contain the water of crystallization. A diameter of about

0947-6539/95/0109-0640 $ 10.00+.25/0 Chem. Eur. J. 1995, 1, No. 9

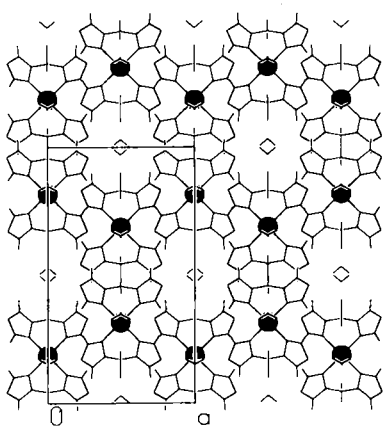

Fig. 9. Crystal packing in **12** with a view on the *ab* plane. The nickel centers are given as black circles, and the ligands and the water of crystallization as stick drawings for a better illustration of the pseudo-hexagonal symmetry of the heavy atoms and the channels formed (PLUTON [11]).

5 Å is estimated between the surrounding nitrogen and hydrogen centers, correspondingly less if the covalent or van der Waals radii of these atoms are taken into account. One might be tempted to invoke self-assembly of the complexes here. The intermolecular interaction responsible in part would have to be the formation of a bridge by the hydrogen bonds of an aqua ligand between two exodentate nitrogen atoms of two neighboring complex molecules (Figs. 7 and 8). In addition, we think of the channel formation as caused by the intimate solvent–complex interactions carried over from solution to the solid phase. The channels could result from the formation of a chain along *c* by hydrogen bonds in the water of crystallization. This water chain is probably of a more continuous, dynamic nature at room temperature and interrupted at low temperature in an ordering process, a phase transition giving the dimeric units (cf. the dynamics and the ordering of the "two-dimensional" water substructure in **6**, demonstrated especially in the case of the nickel complex).[3–5]

X-Ray crystal structure of 13: The structure of **13** is that of a two-dimensional coordination polymer, with the bis(tetrazolyl)borato ligand bridging the octahedrally coordinated nickel atoms through the C–H neighboring N4 atom (Figs. 10 and 11). Two *trans*-coordinated ammine ligands conclude the nickel coordination polyhedron. All Ni–N distances are very similar. The crystal structure does not contain any water of crystallization. There are no voids in this structure which are large enough for solvent molecules, as can be envisioned from Figure 11 and by a free-space/solvent-accessible area calculation with the PLATON program.[11]

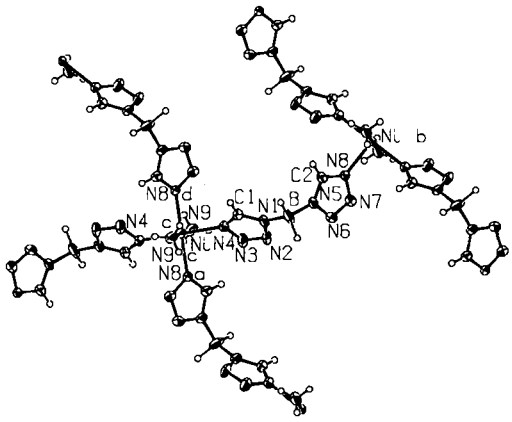

Fig. 10. Detailed metal coordination and atomic numbering scheme in **13** (PLATON-TME plot [11], 50% probability ellipsoids). Selected distances (Å) and angles (°): Ni–N4 2.106(3), Ni–N8 2.117(3), Ni–N9 2.095(4), N4-Ni-N9 90.9(1), N4-Ni-N9c 89.1(1), N4-Ni-N8a 88.3(1), N4-Ni-N8d 91.7(1), N8a-Ni-N9 88.8(1), N8a-Ni-N9c 91.2(2). Symmetry transformations: $a = 1-x,\ ^1/_2-y,\ ^1/_2-z$; $b = 2-x,\ ^1/_2-y,\ ^3/_2-z$; $c = 1-x,\ 1-y,\ 1-z$; $d = 2-x,\ ^1/_2+y,\ ^3/_2-z$.

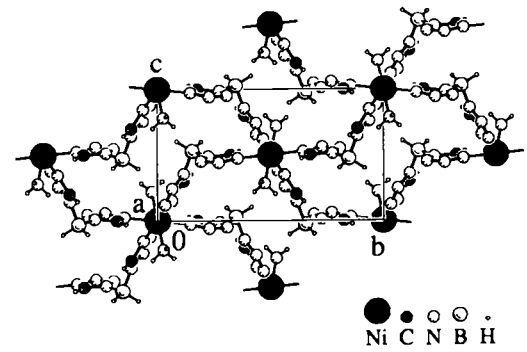

Fig. 11. Structure of the two-dimensional Ni ligand framework in **13** (PLUTON [11]). View from above a layer along *a*. The layers are stacked on top of each other.

The appearance of **13** and its synthesis by two different routes again required the authentication of the single-crystal X-ray structure by comparison with the two microcrystalline bulk samples by X-ray powder diffractometry (Fig. 12).

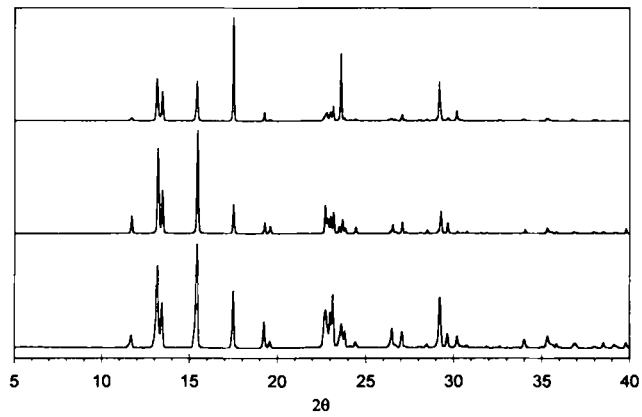

Fig. 12. Top: X-ray powder pattern of a sample of **13** prepared from hexaaquanickel and recrystallized from ammonia [cf. Eq. (3), method 1]. Middle: Simulation from the single crystal data [15]. Bottom: Sample of **13** prepared from hexaamminenickel and crystallized directly from the reaction mixture [cf. Eq. (4), method 2]. The data indicates structural identity; intensity differences are due to texture effects because of a nonrotating sample.

Discussion

Table 3 summarizes the structural features of the various metal complexes of the poly(azolyl)borates **3**–**5** with respect to their mono- or polymeric character and isostructural relationships. It is evident that the respective ligands show a strong preference for a particular structure, regardless of the metal involved. In view of the often isostructural nature of the metal–ligand compounds, the deviations encountered seem at first even more striking. The hydrotris(triazolyl)borato ligand prefers tridentate chelate coordination through the endodentate nitrogen atoms, thus forming molecular complexes from iron to zinc (**6**), with, in the case of zinc, the possibility of a second (linkage) isomer in the form of a coordination polymer (**7**). For manganese a coordination polymer only has been found (**11**). This change cannot be caused by the difference in size of the metal center, as analogous tris(pyrazolyl)borato manganese[16] and zinc chelate derivatives[17] can easily be prepared. Structural data for the dihydrobis(triazolyl)borato ligand is somewhat more scarce, but the difference in structure between the nickel and copper compounds, the former a molecular chelate complex (**12**), the

Table 3. Structural features of metal complexes with modified poly(azolyl)borato ligands [a].

Ligand \ Metal	Mn^{2+} (d^5)	Fe^{2+} (d^6)	Co^{2+} (d^7)	Ni^{2+} (d^8)	Cu^{2+} (d^9)	Zn^{2+} (d^{10})
$HB(C_2H_2N_3)_3$ 3	1-D coord. polym. (11)	molecular chelate complexes (6)				3-D coord. polym. (7)
$H_2B(C_2H_2N_3)_2$ 4	2-D coord. polym. (8)			molecular chelate complex (12) *	1-D coord. polym. (9) *	
$H_2B(CHN_4)_2$ 5	2-D coord. polym. (symmetrical, 10)			2-D coord. polym. (distorted) (13) *	(10') *	2-D coord. polym. (sym., 10)

[a] Bold-framed windows refer to the structures presented in this manuscript. For the other structures, see ref. [3–7]. The same background shading is meant to underscore the isostructural character. Asterisks indicate that the compound has been crystallized from aqueous ammonia or a metal–ammine complex. The Cu complexes exhibit an additional Jahn–Teller distortion. Numbers in bold refer to the schematic structure drawings in the introduction.

latter a coordination polymer (**9**), is not immediately understandable. Finally, in most cases the dihydrobis(tetrazolyl)borate exists solely as a bridging ligand in a highly symmetrical 2-D rhombohedral grid structure (**10**) except for the nickel and copper compounds (**13** and **10'**). Before the nickel structure of **5** was known, the lower symmetry of its copper structure (**10'**) was explained simply by the Jahn–Teller distortion of the central metal.[6] In view of the new results the structural distortion must be ascribed to a different cause.

In the following we will show how the metal–ligand coordination depends upon and can be controlled by i) the nitrogen donor properties and the chelate effect, ii) the electron count at the metal or its ligand-field stabilization, and iii) the crystallization conditions.

The difference between the coordination chemistry of manganese and zinc with the ambidentate ligand **3** and that of the analogous complexes from iron to copper can be traced to the zero ligand-field stabilization energy (LFSE) of the d^5 (high-spin) and d^{10} metal. In the case of Mn^{2+} (high-spin) and Zn^{2+}, no additional energetic driving force results from the LFSE upon substitution of an aqua ligand by a stronger N donor ligand. This fact has been best investigated for the stepwise formation of ethylenediamine complexes and is quantitatively illustrated by a plot of the stability constants as a function of the metal (Fig. 13).[18] The resulting order of stability based on K_1 and K_2 with a (relative) minimum at manganese and zinc and a maximum at copper is also known as the Irving–Williams series.[19]

It is also important to realize that the exchange of an aqua for a poly(azolyl)borato ligand will occur stepwise. If the first donor atom is an endodentate nitrogen, the further exchange may be accelerated by the higher effective concentration of the other *endo* N donors in the vicinity of the metal center according to Schwarzenbach's model[20] to give the well-known chelate effect. Still, the backward reaction which regenerates the hexaaqua complex and the existence of an equilibrium have also to be taken into consideration depending on the energy gain upon substitution of the H_2O ligand, and the large excess of water must be kept in mind. If the first donor atom is an *exo* nitrogen, the reaction can proceed only towards a coordination polymer, whose formation will generally be slower under the diffusion-controlled conditions applied here. Thus, ligand-exchange equilibria can again be formulated. Scheme 1 illustrates this *exo–endo* equilibrium and shows the chelate complexes that form for Fe to Zn, these being the major product for Fe to Cu because of the high stability constants (Fig. 13). Coordination polymers of Fe to Cu with **3** were in part obtained as amorphous precipitates upon rapid admixture of the reactants but were not characterized further.

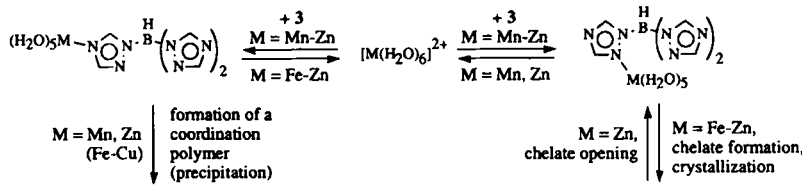

Scheme 1. Proposed equilibria between the exo- and endodentate coordination mode in the complex formation with the hydrotris(triazolyl)borato ligand **3** to explain the observed differences in metal–nitrogen coordination for M = Mn and Zn versus Fe, Co, Ni, and Cu.

Zinc, however, is a metal which is more stable in a tetrahedral environment than the other first-row transition metals; this explains the rather high stability constants K_1 and K_2 despite the d^{10} configuration (Fig. 13). The preferred ammine complex appears to be $[Zn(NH_3)_4]^{2+}$ rather than $[Zn(NH_3)_6]^{2+}$, which is only formed at high ammonia concentrations; hence the constant K_3 for the octahedral complex is much smaller.[18] This helps to explain the initially observed formation of the octahedral molecular chelate complex of zinc with **3** (**6**).[4] Its lower stability allows, however, for an opening of the chelate rings by H_2O and a new *exo* N coordination, most likely from a free ligand in solution. In the end a complete transformation to the 3-D coordination polymer as the apparently thermodynamically more stable isomer results. This therefore leads us to conclude that *exo* N coordination is thermodynamically more stable than the *endo* N–metal interaction.

In the case of manganese, the effect of LFSE is even more pronounced. Substitution of an aqua ligand results only in a small energy gain so that the nitrogen donor characteristics can determine the position of the *exo–endo* equilibrium outlined in Scheme 1. With the exodentate nitrogen atom being the better donor, the equilibrium will be shifted to the left, so that coordination polymers are formed.

An additional hint on the importance of the outlined equilibrium in the case of manganese and zinc is obtained from the reaction rates: while admixture of the reactant solution results in immediate precipitation of Fe, Co, Ni, or Cu, the products

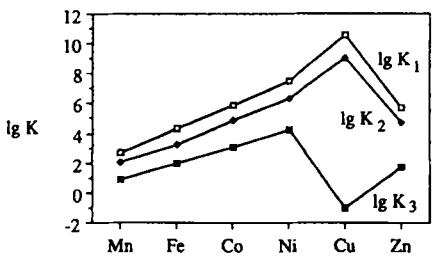

Fig. 13. Stability constants for the stepwise formation of 1:1, 1:2, and 1:3 (aqua)ethylenediamine metal complexes $[M(en)_n(H_2O)_{6-2n}]^{2+}$. Stability constants taken and figure adapted from ref. [18].

0947-6539/95/0109-0642 $ 10.00+.25/0 Chem. Eur. J. 1995, 1, No. 9

precipitate significantly more slowly for Mn and Zn. Thus in the case of the bis(triazolyl)borato ligand (**4**) the change from coordination polymer to molecular chelate complex (structure **8** versus **12**) from manganese to nickel follows the trend in LFSE and is straightforward. However, the fact that the copper derivative (structure **9**) is again a coordination polymer appears to be an anomaly. After all, the LFSE for 1:1 and 1:2 complexes (K_1 and K_2) with a bidentate ligand is highest for copper (Fig. 13). This difficulty is resolved when one takes into account the fact that the crystals of **12** and **9** were obtained from ammoniacal solution or a metal-ammine complex, respectively. Contrary to the above discussion based on Scheme 1, complex formation then does not proceed from a hexaaqua but from ammine-aqua complexes [Eqs. (5) and (6)]. In the case of nickel, the exchange

$$[Ni(NH_3)_4(H_2O)_2]^{2+} + \mathbf{4} \longrightarrow [Ni(\eta^2\text{-}\mathbf{4})(NH_3)_4]^{+} + 2H_2O \longrightarrow \ldots \quad (5)$$

$$[Cu(NH_3)_4(H_2O)_2]^{2+} + \mathbf{4} \longrightarrow [Cu(\eta^1\text{-}\mathbf{4})(NH_3)_4H_2O]^{+} + H_2O \longrightarrow \ldots \quad (6)$$

of H_2O for the stronger bis(triazolyl)borato ligand leads to a gain in LFSE and to the formation of chelate rings. In the tetraamminecopper complex, on the other hand, the four NH_3 ligands are bound very strongly to the central metal with short distances in the equatorial plane because of the Jahn-Teller distortion. This is the reason for the maxima of the stability constants K_1 and K_2 at copper in the Irving-Williams series (cf. Fig. 13).[18, 19] Thus any ligand exchange will have to start at the axial, loosely bound H_2O ligands. Formation of chelate rings from this position through a reorganization of the remaining ligands or through substitution of a *cis* NH_3 ligand might be possible but is energetically highly unfavorable, as is demonstrated by the very small stability constant K_3 (Fig. 13) in the case of the $[Cu(en)_3]^{2+}$ complex ($\log K_3 = -1.0$).[18] More importantly, however, substitution of the weak H_2O ligands in the tetraamminecopper complex by a stronger N donor ligand (even monodentate) is unfavorable to begin with, as can be seen by the stability constant for the pentaamminecopper complex of $\log K_5 = -0.52$.[18] Analogously to the equilibria outlined in Scheme 1, a similar *exo-endo* N equilibrium with a tetraamminecopper ion as intermediate can be formulated, from which crystallization of the thermodynamically more stable *exo* adduct then occurs (see Scheme 2).

For the bis(tetrazolyl)borato ligand (**5**), the two-dimensional coordination polymer is the sole structure so far known; the borate functions as a bridging ligand through the C-H neighboring nitrogen donor. Yet it is interesting to note that highly symmetrical two-dimensional rhombic grid sheets (**10**, orthorhombic crystal system, space group *Cmca*) result when the crystals are grown from water, whereas lower-symmetry distorted 2-D frameworks are obtained when ammonia is involved as a ligand, as has been found in the closely related structures of the nickel and copper derivatives (**13** and **10'**, monoclinic crystal system, space group $P2_1/c$ and $P2_1/a$).[6] We may not yet have a fully proven explanation for this difference in structure based on the crystallization conditions, but for the packing of the metal-ligand complexes, chains, and layers in the water containing crystal phases (the "secondary structure", so to speak) we would like to point to the hydrogen bonds as a possibly important design element already well recognized in organic chemistry[21] and in biological systems[22] but less so in inorganic chemistry.

The symmetrical structure **10** contains two water molecules of crystallization per formula unit. Hydrogen bonding to the aqua ligands at the metal center gives rise to one-dimensional chains of water molecules that run parallel to the 2-D metal-ligand grid sheets; in ref. [6] it was emphasized that the hydrogen bonds along the water chain are invariant with the change in metal, thereby including metals from manganese to zinc and even cadmium. As regards the water chain, we would like to suggest the metaphor of a reinforcing bar for the metal-ligand framework. With ammine ligands completing the metal coordination spheres in the nickel and copper compounds (**13** and **10'**) no water of crystallization is incorporated, possibly owing to the weaker hydrogen-bond forming capability of NH_3. What is observed then is solvent-free crystal packing in the form of a less symmetrical, distorted grid sheet. In view of the increased interest in the controlled synthesis of two- and three-dimensional inorganic materials,[23] hydrogen bonding should not be overlooked as a possible design element also in inorganic chemistry.[24]

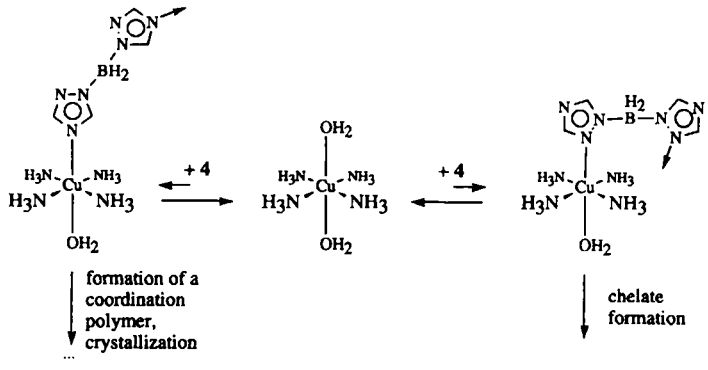

Scheme 2. Proposed equilibria between the exo- and endodentate coordination mode in the initially unfavorable copper complex formation with the dihydrobis(triazolyl)borato ligand (**4**), starting from a tetraamminecopper complex, to explain the formation of the thermodynamically more stable *exo* adduct.

Conclusions

Using modified, potentially ambidentate poly(triazolyl)borates as examples, we have demonstrated how ligand-field stabilization energy can be used to control metal-ligand assembly during the crystallization process to give either chelate complexes or coordination polymers. The choice of the coordinating solvent ligand is an interesting tuning variable which can not only be a decisive factor for the metal-ligand interaction but can also provide a design element for the (secondary) solid-state structure by transferring solvent-solvent interactions from the solution to the solid phase. The nature of the hydrogen-bonding network built up by incorporated solvent molecules can control the conformation assumed by the metal-ligand framework.

Experimental Procedure

Twice distilled or deionized water was used as a solvent. CHN: Perkin-Elmer Series II CHNS/O Analyzer 2400. IR: Nicolet Magna 750. MS: Varian MAT 311 A. Susceptibility measurements: AC susceptometer Lakeshore Model 7000. X-ray powder diffractograms: INEL, $Cu_{K\alpha}$ radiation, quartz monochromator, sample in 0.7 mm glass capillaries on rotating probe head. The potassium salts of **3**-**5** were synthesized from KBH_4 and triazole or tetrazole, respectively, according to refs. [2, 5, 25]. The synthesis of **12** was also described in ref. [5].

$^1_\infty\{[Mn\{\mu\text{-}HB(C_2H_2N_3)_2\}_2(H_2O)_2]\cdot 4H_2O\}$ (**11**): A solution of anhydrous $MnCl_2$ (0.13 g, 1.0 mmol) in degassed H_2O (3 mL) in a Schlenk tube under argon was carefully overlayered with a solution of the potassium salt of **3** (0.50 g, 2.0 mmol) in degassed water (8 mL). Within a few days ill-shaped colorless-to-white crystals formed. The reaction could also be carried out in air, but a brown precipitate formed upon prolonged storage of the crystals under water. The crystal yield lay between 0.30 and 0.40 g (50-67%). M.p.: no visible decomposition to over 500 °C after the

loss of water of crystallization at 100–105 °C. IR (KBr): $\tilde{\nu}$ = 3420 br s (OH), 3137 w (CH), 2505 w–m (BH), 1661 w, 1513 s, 1416 w, 1336 w–m, 1283 m, 1217 vw, 1191 s, 1139 s, 1107 vw, 1078 w, 1061 vw, 1031 vw, 1008 m, 990 m, 976 w, 898 vw, 882 w, 792 sh, 771 sh, 738 m, 677 m–s, 652 sh cm^{-1}. MS (EI, 70 eV, 320 °C), *m/e* (%): 487 (100, $[C]^+$), 419 (27, $[C-C_2H_2N_3]^+$), 417 (13, $[C-C_2H_2N_3-2H]^+$), 350 (38, $[C-2C_2H_2N_3-H]^+$), 349 (19, $[C-2C_2H_2N_3-2H]^+$), 323 (3, $[C-2C_2H_2N_3-H-HCN]^+$), 271 (66, $[C-HB(C_2H_2N_3)_3]^+ = [Mn\{HB(C_2H_2N_3)_3\}]^+$), 202 (28, $[Mn\{HB(C_2H_2N_3)_3\}-C_2H_2N_3-H]^+$), 175 (39, $[Mn\{HB(C_2H_2N_3)_3\}-C_2H_2N_3-H-HCN]^+$), 69 (32, $[C_2H_3N_3]^+$). Magnetic moment: $\mu = 5.6\mu_B$ (295 K), Curie–Weiss constant $\theta = 11$ K. $C_{12}H_{26}B_2MnN_{18}O_6$ (595.02): calcd. C 24.22, H 4.40, N 42.37; found C 24.72, H 3.94, N 42.24.

$^2_\infty$\{[Ni{μ-H$_2$B(CHN$_4$)$_2$}$_2$(NH$_3$)$_2$]\} (**13**):

Method 1: A solution of $NiCl_2 \cdot 6H_2O$ (0.24 g, 1.0 mmol) in water (10 mL) was carefully overlayered in a test tube with a solution of the potassium salt of **5** (0.38 g, 2.0 mmol) in water (20 mL). No crystalline material but a voluminous amorphous violet precipitate formed from which the clear supernatant solution was decanted; the solid was washed with water and completely dissolved in concentrated aqueous ammonia (25%) to form a clear light pink-violet solution. The solvent was slowly allowed to evaporate. During the process a pink-violet microcrystalline material formed which proved on analysis to be **13** (yield 0.18 g, 46%). The crystals were, however, not of a suitable quality for single-crystal X-ray diffraction studies.

Method 2: A blue solution of $[Ni(NH_3)_6]Cl_2$ (0.23 g, 1.0 mmol) in water (10 mL) was carefully overlayered in a test tube with a solution of the potassium salt of **5** (0.38 g, 2.0 mmol) in water (20 mL). Some amorphous material precipitated in this process. Slow diffusion of the starting compounds then led to the formation of **13** as analytically pure crystals. Crystal growth started within 2 d, and the reaction and process of crystallization appeared to be concluded within 10 d. The single crystals obtained by this route were small, yet suitable for an X-ray study (yield 0.26 g, 66%).

Infrared spectroscopy as well as X-ray powder diffraction proved the chemical and structural identity of the samples obtained by the two routes. M.p. > 250 °C (undetermined; for a caveat on the thermal stability of bis(tetrazolyl)borate, see ref. [6]). IR (KBr): $\tilde{\nu}$ = 3365 br s (NH), 3279 w, 3166 m (CH), 3127 m (CH), 2495 m (BH), 2433 m (BH), 1616 w, 1496 m, 1481 s, 1390 w, 1280 w, 1266 w, 1229 m–s, 1197 m, 1190 m, 1163 m–s, 1146 m, 1118 w, 1102 vs, 1037 m, 1025 vw, 1010 w, 986 w, 903 w, 869 w, 742 vw, 708 m–s, 681 vw, 659 vw, 643 m–s, 603 w cm^{-1}. Magnetic moment: $\mu = 3.0\mu_B$ (295 K), Curie–Weiss constant $\theta = -1.7$ K. $C_4H_{14}B_2NiN_{18}$ (394.60): calcd. C 12.17, H 3.58, N 63.89; found C 12.53, H 3.55, N 63.52.

Table 4. Crystal data for compounds 11–13.

Compound	11	12	13
formula	$C_{12}H_{26}B_2MnN_{18}O_6$	$C_8H_{20}B_2N_{12}NiO_4$	$C_4H_{14}B_2N_{18}Ni$
M_r (g mol^{-1})	595.06	428.70	394.66
crystal size (mm)	0.5 × 0.1 × 0.1	0.4 × 0.1 × 0.1	0.1 × 0.15 × 0.15
T (K)	293(2)	160(2)	293(2)
diffractometer	STOE	CAD4	Turbo CAD4 with rotating anode generator
radiation/λ (Å)	$Mo_{K\alpha}$/0.71069	$Mo_{K\alpha}$/0.71069	$Cu_{K\alpha}$/1.5418
monochromator	graphite	graphite	nickel filter
scan type, 2θ range	ω, 4–50°	ω-2θ, 4–68°	ω, 11–120°
h; k; l range	−10,10; −10,10; 0,12	0,13; 0,23; 0,12	−8,8; 0,14; 0,8
crystal system	triclinic	orthorhombic	monoclinic
space group	P1 (no. 2)	$Cmc2_1$ (no. 36)	$P2_1/c$ (no. 14)
a (Å)	8.914(3)	11.549(3)	7.8635(9)
b (Å)	9.163(3)	20.112(3)	13.353(1)
c (Å)	10.513(3)	7.615(2)	8.0733(7)
α (°)	103.78(2)	90	90
β (°)	100.28(3)	90	105.69(1)
γ (°)	117.69(2)	90	90
V (Å^3)	695.4(4)	1768.8(7)	816.1(1)
Z	1	4	2
$D_{calcd.}$ (g cm^{-3})	1.421	1.610	1.606
F(000) (electrons)	307	888	404
μ (cm^{-1})	5.37	11.4	20.4
absorption correction	DIFABS [a]	DIFABS [a]	DIFABS [a]
max.; min.; mean	1.143; 0.821; 0.990	1.269; 1.071; 1.138	1.893; 0.719; 1.020
measured reflections	2459	1716	1103
unique reflections (R_{int})	2298 (0.019)	880 (0.041)	1015 (0.098)
data for refinement (n)	2284	863	1015
parameters refined (p)	217	146	140
max; min Δρ [b] (e Å^{-3})	0.23; −0.25	0.36; −0.40	0.28; −0.28
$R1$; $wR2$ [c] [$I > 2\sigma(I)$]	0.0344; 0.0700	0.0305; 0.0743	0.0364; 0.0879
GOF on F^2 [d]	0.661	1.005	0.797
weighting scheme, w; a; b [e]	0.000; 0.000	0.039; 5.0514	0.0635; 1.6875
Flack parameter [f]	–	0.01(3)	–

[a] Empirical absorption correction [28]. [b] Largest difference peak and hole. [c] $R1 = (\sum||F_o| - |F_c||)/\sum|F_o|$; $wR2 = [\sum[w(F_o^2 - F_c^2)^2]/\sum[w(F_o^2)^2]]^{1/2}$. [d] GOF = $[\sum[w(F_o^2 - F_c^2)^2]/(n-p)]^{1/2}$. [e] $w = 1/[\sigma^2(F_o^2) + (a \times P)^2 + b \times P]$ where $P = (\max(F_o^2 \text{ or } 0) + 2 \times F_c^2)/3$. [f] Absolute structure parameter [29].

X-Ray structure determinations of 11–13: Structure solution was performed by direct methods (SHELXS-86 [26]). Refinement: Full-matrix least-squares on F^2 (SHELXS-93 [26]); all atomic positions including those of the hydrogen atoms found and refined (non-hydrogen atoms with anisotropic temperature factors). Crystal data are listed in Table 4 [27].

Acknowledgements: This work was supported by the Deutsche Forschungsgemeinschaft (grant Ja 466/4-1), the Fonds der Chemischen Industrie, and the Freunde der TU Berlin. We express our appreciation and thanks to Prof. H. Schumann for his continuous, generous, and encouraging support.

Received: February 20, 1995 [F90]

[1] Reviews: S. Trofimenko, *Chem. Rev.* **1993**, *93*, 943–980; P. K. Byers, A. J. Canty, R. T. Honeyman, *Adv. Organomet. Chem.* **1992**, *34*, 1–65. K. Niedenzu, S. Trofimenko, *Top. Curr. Chem.* **1986**, *131*, 1–37; S. Trofimenko, *Progr. Inorg. Chem.* **1986**, *34*, 115–210.
[2] C. Janiak, L. Esser, *Z. Naturforsch. Teil B* **1993**, *48*, 394–396.
[3] C. Janiak, *J. Chem. Soc. Chem. Commun.* **1994**, 545–547.
[4] C. Janiak, H. Hemling, *J. Chem. Soc. Dalton Trans.* **1994**, 2947–2952.
[5] C. Janiak, T. G. Scharmann, H. Hemling, D. Lentz, J. Pickardt, *Chem. Ber.* **1995**, *128*, 235–244.
[6] C. Janiak, T. G. Scharmann, K.-W. Brzezinka, P. Reich, *Chem. Ber.* **1995**, *128*, 323–327.
[7] C. Janiak, *Chem. Ber.* **1994**, *127*, 1379–1385.
[8] J.-M. Lehn, *Angew. Chem.* **1990**, *102*, 1347–1362; *Angew. Chem. Int. Ed. Engl.* **1990**, 29, 1304–1319.
[9] A preliminary account of the synthesis of **12** has been mentioned in ref. [5].
[10] A. Weiss, H. Witte, *Magnetochemie*, Verlag Chemie, Weinheim, **1973**. F. E. Mabbs, D. J. Machin, *Magnetism and Transition Metal Complexes*, Chapman and Hall, London, **1973**.
[11] A. L. Spek, *PLATON-93* and *PLUTON-92* graphics program, University of Utrecht, The Netherlands, **1993** and **1992**, respectively; A. L. Spek, *Acta Crystallogr. Sect. A*, **1990**, *46*, C34.
[12] C. Janiak, T. G. Scharmann, P. Albrecht, F. Marlow, submitted for publication in *J. Am. Chem. Soc.*
[13] W. Saenger, K. Lindner, *Angew. Chem.* **1980**, *92*, 404–405; *Angew. Chem. Int. Ed. Engl.* **1980**, *19*, 398–399.
[14] T. Steiner, W. Saenger, *J. Am. Chem. Soc.* **1993**, *115*, 4540–4547. G. R. Desiraju, *Acc. Chem. Res.* **1991**, *24*, 290–296. R. B. Helmholdt, W. Hinrichs, J. Reedijk, *Acta Cryst.* **1987**, *C43*, 226–229.
[15] X-ray powder simulation with the program *FullProf* by J. Rodriguez-Carvajal, Institute Laue Langevin, Grenoble, France.
[16] M. K. Chan, W. H. Armstrong, *Inorg. Chem.* **1989**, *28*, 3777–3779.
[17] R. Alsfasser, A. K. Powell, S. Trofimenko, H. Vahrenkamp, *Chem. Ber.* **1993**, *126*, 685–694. S. Trofimenko, *J. Am. Chem. Soc.* **1967**, *89*, 6288–6294.
[18] L. E. Orgel, *An Introduction to Transition-Metal Chemistry: Ligand Field Theory*, Methuen, London, **1960**, ch. 5, p. 80–83. M. Gerloch, E. C. Constable, *Transition Metal Chemistry*, VCH, Weinheim, **1994**, ch. 8, p. 161–165.
[19] E. H. Irving, R. J. P. Williams, *Nature* **1948**, *162*, 746–747; *J. Chem. Soc.* **1953**, 3192–3210.
[20] G. Schwarzenbach, *Helv. Chim. Acta* **1952**, *35*, 2344–2359.
[21] M. C. Etter, *J. Phys. Chem.* **1991**, *95*, 4601–4610.
[22] *Water and Biological Macromolecules* (Ed.: E. Westhoff), MacMillan, London, **1993**. G. A. Jeffrey, W. Saenger, *Hydrogen Bonding in Biological Structures*, Springer, New York, **1991**, and references therein. R. L. Harlow, *J. Am. Chem. Soc.* **1993**, *115*, 9838–9839.
[23] Ed.: T. Bein, *Supramolecular Architecture, Synthetic Control in Thin Films and Solids, ACS Symposium Series* **1992**, *499*.
[24] D. Mootz, H. Rütter, R. Wiskemann, *Z. Anorg. Allg. Chem.* **1994**, *620*, 1509–1513. K.-M. Park, R. Kuroda, T. Iwamoto, *Angew. Chem.* **1993**, *105*, 939–941; *Angew. Chem. Int. Ed. Engl.* **1993**, *32*, 884–886.
[25] G. G. Lobbia, F. Bonati, P. Cecchi, *Synth. React. Inorg. Met. Org. Chem.* **1991**, *21*, 1141–1151. S. Trofimenko, *J. Am. Chem. Soc.* **1967**, *89*, 3170–3177. S. Trofimenko, *Inorg. Synth.* **1970**, *12*, 99–106.
[26] G. M. Sheldrick, *SHELXS-93*, Program for Crystal Structure Refinement, Göttingen, **1993**; *SHELXS-86*, Program for Crystal Structure Solution, Göttingen, **1986**.
[27] Further details of the crystal structure investigations may be obtained from the Fachinformationszentrum Karlsruhe, D-76344 Eggenstein-Leopoldshafen (Germany), on quoting the depository numbers CSD-401874 (for **11**), CSD-401875 (**12**), and CSD-401876 (**13**).
[28] N. G. Walker, D. Stuart, *Acta Crystallogr. Sect. A*, **1983**, *39*, 158–166.
[29] H. D. Flack, *Acta Crystallogr. Sect. A*, **1983**, *39*, 876–881.